Journal of Power Sources 195 (2010) 7415–7425

Contents lists available at ScienceDirect

Journal of Power Sources

journal homepage: www.elsevier.com/locate/jpowsour

Aging of the $LiFePO_4$ positive electrode interface in electrolyte

Nicolas Dupré*, Jean-Frédéric Martin, Jeremy Degryse, Vincent Fernandez, Patrick Soudan, Dominique Guyomard

Institut des Matériaux Jean Rouxel, 2 rue de la Houssinière, BP 32229, F-44322 Nantes Cedex 3, France

ARTICLE INFO

Article history:
Received 16 November 2009
Received in revised form 10 May 2010
Accepted 25 May 2010
Available online 31 May 2010

Keywords:
Lithium batteries
$LiFePO_4$
Cathode
Surface
Aging

ABSTRACT

The evolution of lithium-containing species on the surface of grains of 500 nm $LiFePO_4$ and 100 nm carbon-coated $LiFePO_4$ materials during the aging process in $LiPF_6$ electrolyte has been followed using coupled ^{7}Li MAS NMR, EIS (Electrochemical Impedance Spectroscopy) and XPS for materials synthesized with and without carbon coating.

$LiFePO_4$ undergoes surface reactivity upon immersion in classical $LiPF_6$ electrolyte, although its open circuit voltage (~3.2 V) lies in the thermodynamical stability voltage range. The evolution of the NMR signal shows that the reaction of formation of the interphase is very slow as no evidence of passivation could be found even after 1 month of contact with the electrolyte. ^{7}Li MAS NMR combined with XPS indicates that carbon coating has a strong protective role towards formation of surface species on the material and hinders iron dissolution at elevated temperature. Coupled NMR, EIS and XPS experiments showed that the surface of the material grains is not covered by an homogenous layer. Increasing the storage temperature from 25 °C to 55 °C promotes the formation of organic species on the surface, most probably covering inorganic species such as LiF, Li_xPF_y and $LiPO_yF_z$. No evidence of the formation of a resistive film is deduced from the evolution of EIS measurements. The interphase growth can accelerate the degradation of the electrochemical performance, leading to a loss of electrical contact within the electrode.

1. Introduction

Lithium batteries are now the prevailing rechargeable system, they are used in many portable electronic device such as cell phones and computers. Their long lifetime as well as their energy density higher than any other rechargeable batteries assured them such a wide use. The phospho-olivine $LiFePO_4$ is currently under extensive studies and has become one of the most promising candidate for hybrid/electric vehicle propulsion due to its low cost, low toxicity, high thermal stability and high specific capacity of 170 mAh g^{-1}. Recently, the work in progress concerning the enhancement of the electrochemical performance of $LiFePO_4$ has accomplished several important steps. In particular, the poor intrinsic electronic conductivity has been circumvented by using synthesis method yielding carbon-coated particles [1–5]. In parallel, the reduction of particles size ensures an efficient network and a good accessibility of the active material to lithium ions and electrons and allows achieving high cycling rates retaining specific capacities close to theoretical value [6,7].

Decreasing the particle size of any electrode material leads to an increase of its surface area and thus to a subsequent amplification of the parasitic reactions taking place at the interface between the active material surface and the electrolyte. Therefore, in order to avoid catalyzed reactions leading to the deterioration of the active material [8–10] or the formation of a resistive layer from electrolyte decomposition products [11–15], understanding and monitoring the evolution of the interphase are of great importance. Moreover, the experimental conditions of formation, growth and modification as well as the intimacy of the interactions between the surface layer and the surface of active material are still unclear [16–20]. In particular, the beneficial or hindering role played by the interphase(s) is yet to address. Attempts to answer these issues are not a straightforward task due to experimental complications including the low amount of surface species that form and the high sensitivity of the interphase towards ambient atmosphere when using ex situ characterization techniques.

$LiFePO_4$ is believed to be chemically inert upon immersion in electrolyte, then, few studies deal with interphase evolution of $LiFePO_4$ electrode material upon its operation in a lithium battery. Concerning the species formed on the surface of grains of active material, Herstedt et al. [21] did not observe any organic product such as polycarbonates, polymers or Li alkyl carbonates usually found in the case of oxides. Only products from decomposition of

* Corresponding author. Tel.: +33 2 40 37 39 33; fax: +33 2 40 37 39 95.
E-mail address: nicolas.dupre@cnrs-imn.fr (N. Dupré).

0378-7753/$ – see front matter © 2010 Elsevier B.V. All rights reserved.
doi:10.1016/j.jpowsour.2010.05.042

the $LiPF_6$ electrolyte were detected and no correlation with the electrochemical performance could be made. However, Koltypin et al. [14] indicated a decrease of the performance, demonstrated by an increase of the electrode resistance upon storage, as well as the Fe dissolution at elevated temperature. It becomes then necessary to follow the formation and evolution of surface species as a function of time and temperature in order to address the underlying issue of the stability of the surface of $LiFePO_4$ and the role of the interphase on the electrochemical performance.

In this paper, we study the influence of the presence of a carbon coating on the formation and growth of the powder $LiFePO_4$/electrolyte interphase during aging at two temperature, ambient and 55 °C. Species formed on the surface are monitored using ^{7}Li MAS NMR combined with XPS and Electrochemical Impedance Spectroscopy. MAS NMR is an extremely useful, but unusual, technique to follow interface evolution, which we develop in our group [22–25]. Complementary to XPS, which is a local technique, depending on the thickness of the sample but gives precise chemical information, ^{7}Li MAS NMR is a quantitative technique probing the surface of the complete sample and therefore allowing the monitoring of the interphase evolution.

2. Experimental

The $LiFePO_4$ samples used for this study have been obtained through methods described elsewhere. A sol–gel route, proposed by Dominko et al. [26] and involving ferric citrate leads to a carbon coating of the grains of active materials ($LiFePO_4$–C) corresponding to approximatively 6 wt%. The second employed synthesis route [6] in aqueous media allows obtaining a material without any carbon coating ($LiFePO_4$). The obtained pristine samples were kept in a closed vial in ambient atmosphere.

XRD data were collected ($\lambda_{CuK\alpha}$) with a $\theta/2\theta$ BRUKER D5000 diffractometer equipped with a linear MOXTEK detector, using a scan step of 0.01° (2θ) for 10 s.

A first series of samples have been obtained by simple soaking in 1 M $LiPF_6$ in EC/DMC electrolyte for various durations: 3 days, 2 weeks and 1 month, at ambient temperature and 55 °C. After aging, they were centrifuged, rinsed once with DMC and dried under vacuum. The resulting samples were stored under argon.

^{7}Li NMR measurements were carried out at room temperature on a Bruker Avance-500 spectrometer (B_0 = 11.8 T, Larmor frequency ν_0 = 194.369 MHz in ^{7}Li resonance). Single-pulse MAS spectra were obtained by using a Bruker MAS probe with a cylindrical 2.5-mm o.d. zirconia rotor filled with approximately 10 mg of material. Spinning frequencies up to 15 kHz were utilized. A short single-pulse length of 1 μs corresponding to a non-selective $\pi/2$ pulse was used. Recycle time was in the 0.5–60 s range and a spectrometer dead time (preacquisition delay) of 4.5 μs was used before each acquisition. Such experimental conditions were selected in order to detect selectively Li nuclei in surface diamagnetic species and not Li incorporated within the paramagnetic bulk of active material [22–25,27]. The isotropic shifts, reported in parts per million, are relative to an external 1 M solution of LiCl solution set at 0 ppm. In order to perform a quantitative analysis, the different spectra have been analyzed considering the total integrated intensity of the signal for each sample. All parameters were kept as constant as possible for each series of NMR measurements: number of scans, probe tuning process, spinning frequency, etc. The spectra displayed in this work were normalized taking into account the number of scans and the mass of sample.

X-ray photoelectron spectroscopy (XPS) data have been collected using a Kratos Ultra Axis spectrometer. The X-ray source is MgK working at 1253.6 eV and the spot size is 0.7 mm × 0.3 mm. Special care has been taken in the preparation and transfer of the samples. A special air-tied sample holder has been used to transfer the samples from the glove box to the spectrometer in order to avoid any extra reaction with oxygen and/or moisture. Semi-quantitative XPS analysis has been performed using pseudo-Voight function constrained by full width at half-maximum (FWHM) ranges typical of each element. The quality of the initial surface was confirmed by an experimental M/O ratio close to the theoretical one.

Galvanostatic cycling was performed using Swagelok cells and MacPile system at a $C/10$ rate. A slurry of the electrode powder in *n*-methyl-pyrolidinone (NMP) was deposited on a 1 cm^2 aluminum disk and then dried under vacuum at 100 °C for 24 h. Electrodes were constituted of 75 wt% of active material, 20 wt% of ketjenblack carbon and 5 wt% poly-vinylidene di-fluoride (PVdF). For cycling experiments on aged samples, electrodes of pristine materials were made first, and then aged in a complete cell configuration at 25 °C or 55 °C. After aging, electrodes were recovered, rinsed and cycled in a cell with fresh electrolyte and fresh lithium anode. In order to evaluate the specific capacity loss, the same mass of active material was considered.

Electrochemical Impedance Spectroscopy (EIS) measurements (from 50 mHz to 200 kHz) were obtained using a VMP/Z apparatus (Bio-logic, France). A home-made Swagelok-type three electrodes cell was used. The negative electrode was made of a disk of lithium metal. The reference electrode consists of a ring of lithium metal surrounding the working electrode. Measurements have been performed at the end of a 5 h relaxation rest. It was chosen to normalize the results with respect to the specific surface of the studied materials to take into account their difference of surface in contact with the electrolyte. Although it is not completely exact since the electrochemical surface cannot be known, it allows to take into account the effect of grain size and surface rugosity.

For iron dissolution tests, 50 mg of pristine materials were stored in closed vials, containing 10 mL of a 1 M $LiPF_6$ in EC/DMC electrolyte under Ar atmosphere. The solution was centrifuged and removed after a period of storage at 25 °C or 55 °C and analyzed by ICP for the presence of iron.

3. Results and discussions

3.1. Characterization of pristine samples

Fig. 1 exhibits the XRD patterns obtained for the samples synthesized through the two chosen methods. In each case, the diffraction peaks are in full accord with the ordered $LiFePO_4$ olivine structure indexed in the orthorhombic *Pnma* space group and no evidence of impurity phases often seen such as Li_3PO_4 could be observed. The Rietveld refinements for the two types of sample gave the following lattice parameters: a = 10.341(2), b = 6.013(1), c = 4.696(1) Å and a = 10.324(2), b = 6.005(1), c = 4.690(1) Å, for $LiFePO_4$ and $LiFePO_4$–C, respectively, close to the reported data for ordered $LiFePO_4$ (a = 10.334, b = 6.008 and c = 4.693 Å [28]). No diffraction response of the carbon coating was detected due to its low content and amorphous state.

The powder morphologies of the obtained products are shown in Fig. 2. The two materials display completely different surface morphologies as $LiFePO_4$ is made of aggregates (20–30 μm) of approximately 400–500 nm grains and $LiFePO_4$–C exhibits a rougher aspect of smaller grains of approximately 100–200 nm organized in aggregates of size comparable to those found for the non-carbon-coated material (20–30 μm). BET measurements gave specific surfaces of 6 and 30 m^2 g^{-1} respectively for $LiFePO_4$ and $LiFePO_4$–C. The value obtained for the carbon-coated material includes the contribution from the carbon. It is not possible to separate the specific surface due to the carbon coating from the

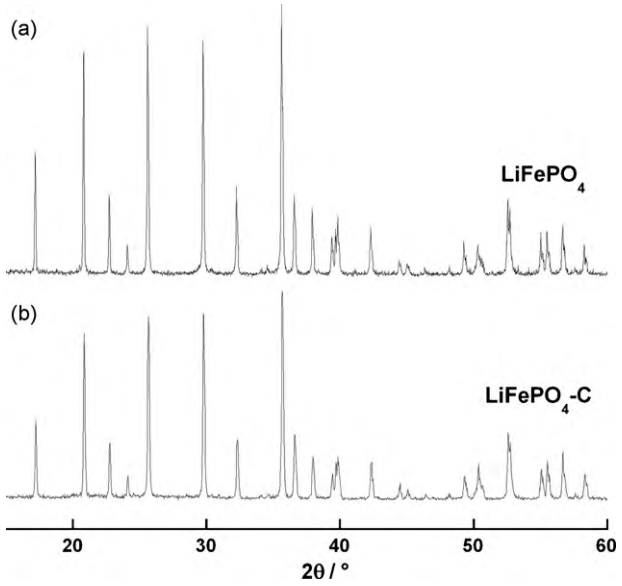

Fig. 1. XRD patterns of $LiFePO_4$ (a) and $LiFePO_4$–C (b), synthesized by an aqueous route and a sol–gel method, respectively.

specific surface due to $LiFePO_4$. Percentages of 3 and 6% of Fe(III) were deduced from Mössbauer measurements respectively for the non-carbon-coated and the carbon-coated materials. Both $LiFePO_4$ samples were evaluated for their reversible Li extraction properties. The corresponding specific capacities obtained at a *C*/10 regime are displayed in Fig. 3. Specific capacity observed for the carbon-coated material is close to published values [6,27] although slightly lower

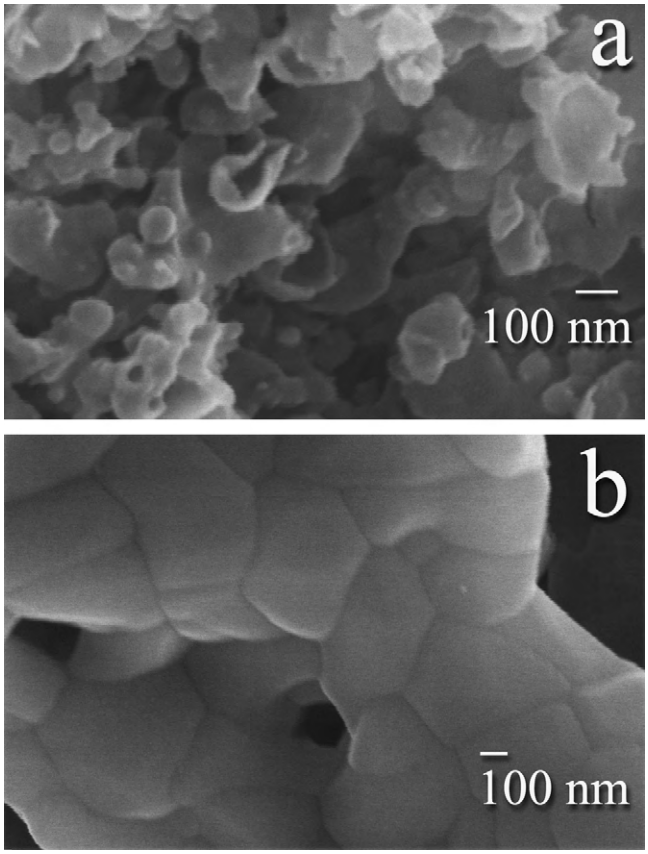

Fig. 2. SEM pictures of $LiFePO_4$–C (a) and $LiFePO_4$ (b).

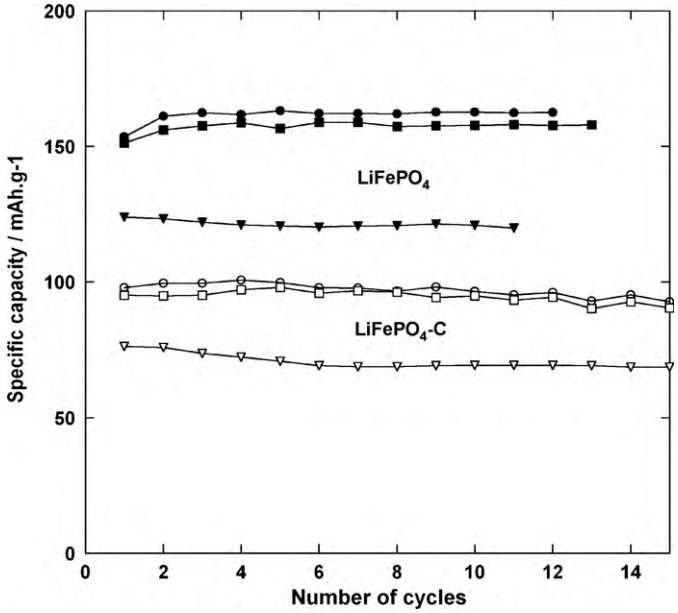

Fig. 3. Specific capacities as a function of the number of cycles for $LiFePO_4$ before aging (circles) in $LiPF_6$ in 1 M EC/DMC, after 1 month aging at 25 °C (open squares) and at 55 °C (open triangles); $LiFePO_4$–C before aging (dots), after 1 month aging at 25 °C (black squares) and at 55 °C (black triangles) at a *C*/10 regime.

(160 mAh g^{-1}), as the electrode formulation was not optimized. As expected, the non-carbon-coated material exhibit significantly lower performance due to the absence of conductive carbon coating and larger grain size, in agreement with published data [29].

3.2. Aging at 25 °C

Fig. 4 shows ^{7}Li MAS NMR spectra for $LiFePO_4$–C (a) and $LiFePO_4$ (b) after various contact durations with $LiPF_6$ electrolyte (1 M EC/DMC). ^{7}Li MAS NMR spectra of the pristine material in contact with ambient atmosphere were published elsewhere previously [30] and very little amount of diamagnetic surface species containing lithium could be detected. For each aged sample, a signal appears at −1 ppm and therefore is assigned to the diamagnetic lithium species formed on the surface from electrolyte contact. Tucker et al. [31] observed a ^{7}Li MAS NMR signal at −8 ppm assigned to lithium within the active material. This observation was performed at low magnetic field (2.4 MHz) allowing the observation of lithium nearby the Fe^{2+} ($S = 2$) and possibly some surface Fe^{3+} ($S = 1/2$ or 5/2) paramagnetic centres. Since our experiments were done at higher magnetic field (11.8 MHz) and due to the extremely strong dipolar interaction between lithium nuclear spin and unpaired electrons spins [32], the corresponding signal cannot be observed. In addition, as the signal intensity changes as a function of the contact duration with electrolyte and temperature, the observed signal corresponds clearly to lithium-containing surface species. The clear evolution of the NMR signal with contact duration also rules out the hypothesis of detecting only dried electrolyte on the surface. In such a case a signal of similar intensity would be observed for all the samples since the same drying protocol has been applied to all of them. The isotropic resonance is quite broad most probably due to chemical shift distribution as well as to the presence of the paramagnetic active material shortening the T_2 of the observed signal. Therefore, it might include several lithium compounds that can be found on the surface of cathode materials such as LiF, $Li_xP_yF_z$ and/or $Li_xPO_yF_z$ [25,20]. For the two types of samples, carbon-coated and carbon free, the amount of surface lithium species increases continuously with the contact

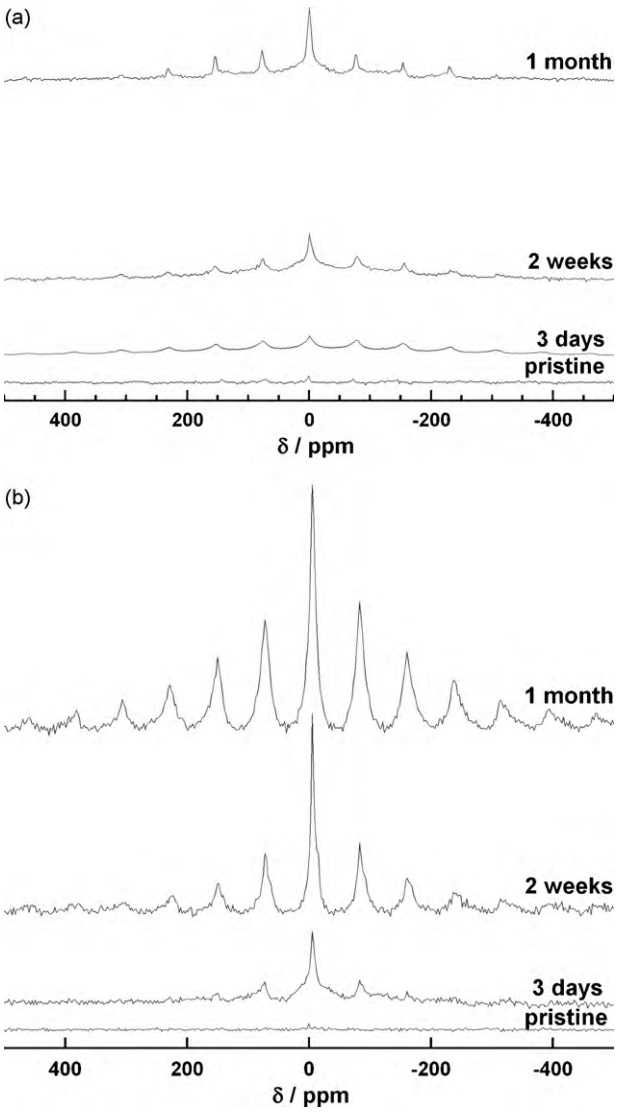

Fig. 4. Normalized ^{7}Li MAS NMR spectra of $LiFePO_4$–C (a) and $LiFePO_4$ (b) soaked in $LiPF_6$ 1 M in EC/DMC for various durations at 25 °C: pristine, 3 days, 2 weeks and 1 month.

duration indicating the slow kinetics of formation of the interphase. Indeed, after one month of contact, the detected NMR signal for $LiFePO_4$ has increased significantly compared to the sample soaked for two weeks (Fig. 4b). Concerning this carbon-free material, the integration of the NMR signal indicates that the amount of surface lithium is multiplied by 1.89 from 3 days to 2 weeks and by 2.60 from 2 weeks to 1 month which is close to a linear progression (Fig. 5), indicating that a possible passivation is not yet achieved. In addition, it emphasizes the much slower kinetics of reaction of the iron phosphate compared to layered transition metal oxides such as $LiNi_{0.5}Mn_{0.5}O_2$ [25,30] for which the reaction with the electrolyte seems to reach a plateau after few minutes of contact. Moreover, the detected signal for the carbon-free $LiFePO_4$ is significantly more intense than that for $LiFePO_4$–C, as it can be seen from Fig. 5, although the specific surface measured was six times smaller and average grain size twice bigger (400–500 nm) for the carbon-free material. In addition the carbon-coated $LiFePO_4$ displays a much rougher surface (Fig. 2a) compared to the smooth surface (Fig. 2b) that can be observed for the carbon-free $LiFePO_4$. Fig. 5 displaying the integration of the NMR signal, indicates a slower increase of the amount of lithium species in the interphase for the carbon-coated material. As a matter of fact, the amount of

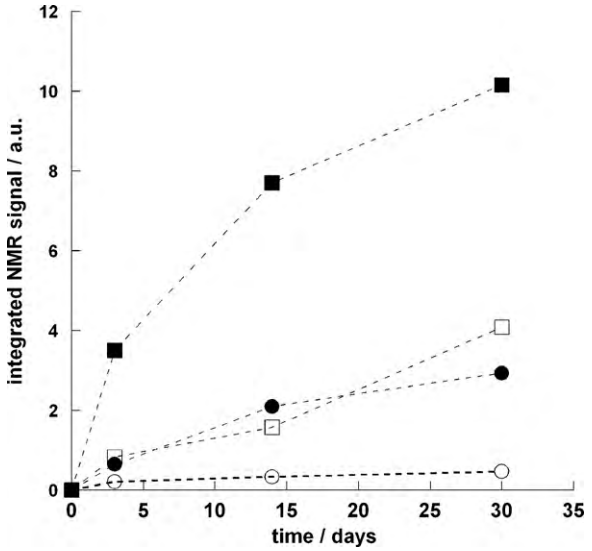

Fig. 5. Evolution of the integrated intensity of normalized ^{7}Li MAS NMR signal of $LiFePO_4$–C (circles) and $LiFePO_4$ (squares) soaked in $LiPF_6$ 1 M in EC/DMC for various durations at room temperature (open symbols) and at 55 °C (black symbols). Note that $LiFePO_4$–C sample has a 5 times larger BET surface area.

surface lithium increases by a factor of approximately 1.57 from 3 days to 2 weeks and 1.43 from 2 weeks to 1 month. These results indicate the strong protective role of the carbon coating towards the formation of a lithiated interphase on the surface of the electrode, counteracting the expected effect of a smaller grain size and higher surface/volume ratio.

In parallel of ex situ ^{7}Li MAS NMR studies, the evolution of the two $LiFePO_4$ samples has been followed by Electrochemical Impedance Spectroscopy (EIS), which corresponds to in situ experiments. For each tested electrode, the Nyquist diagram exhibits one semi-circle at high frequency from which a capacitance in the range 10–20 $\mu F\,cm^{-2}$ can be calculated, depending on the sample. It corresponds to the typical order of magnitude of double layer capacitance (10–50 $\mu F\,cm^{-2}$). Nevertheless, in order to rule out other hypothesis such as the intergrain contact resistance within the composite electrode and the presence of a resistive film on the surface of the grains of active material, a series of experiments, described below, have been performed. In a first step, an electrode has been pressed at 9 tons in order to enhance the electrical contact between grains. The Nyquist diagrams displayed in Fig. 6 indicate only a small contribution of the intergrain contact resistance (which, therefore, cannot be the main detected phenomenon) to the initial overall resistance. In a second step, we changed the concentration and the nature of the electrolyte (Fig. 6). The decrease of the resistance when the Li concentration increases from 0.04 M to 1 M supports the hypothesis of a charge transfer phenomenon. Indeed, in this case, increasing the concentration in Li salt of the electrolyte, considering the same electrode and therefore the same exposed surface, will enhance the charge transfer. In the case of a resistive film, no evolution of the resistance would be expected. Thus, considering these results, we assume that the observed semi-circle corresponds to an interfacial phenomenon and mostly here to a charge transfer phenomenon.

The Nyquist diagrams obtained for various contact durations with the 1 M $LiPF_6$ electrolyte do not show any evolution for both compounds from 1 min to 2 weeks (Fig. 7). Therefore, no evidence of formation of a resistive surface film could be observed as no additional semi-circle appears. Moreover, no hindering of the charge transfer that would reflect a deterioration of the electrode was noticed. These results are in direct agreement with the very good stability of electrochemical performances of $LiFePO_4$ in moderate

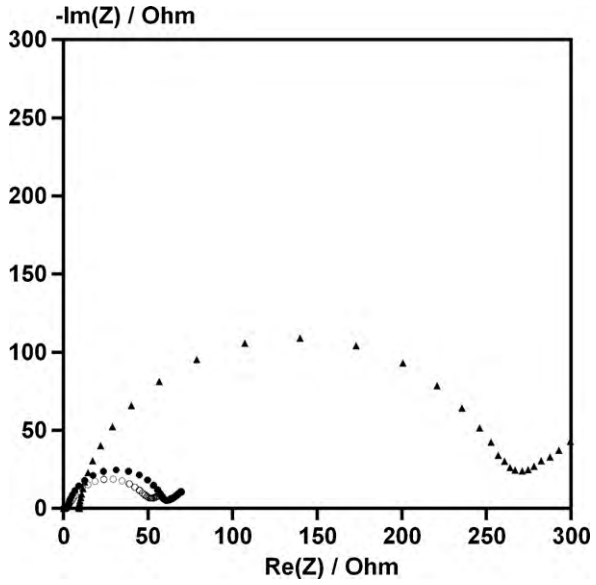

Fig. 6. Nyquist diagrams at 25 °C for $LiFePO_4$ electrode (dots), $LiFePO_4$ electrode pressed under 9 tons (circles) in $LiPF_6$ 1 M and $LiFePO_4$ electrode in $LiPF_6$ 0.004 M (triangles).

conditions of storage (see Fig. 3 at 25 °C). If a resistive film were formed on the surface of the electrode material, a detrimental effect should be observed on the discharge capacity for a fixed cycling rate. However, if the expected new semi-circle related to a resistive film has a time constant close to that of the charge transfer reaction, two semi-circles would be hardly distinguished. Therefore, it is difficult to completely rule out a small contribution of such film. Nevertheless, EIS results do not follow the same trend as the NMR evolution. Such apparent discrepancy will be discussed below.

In order to monitor the state of the surface after aging of the electrode, XPS experiments have been performed on samples exposed to the electrolyte for 1 month (Figs. 8 and 9). In addition, XPS experiments were performed on pristine materials to investigate the nature of the surface species found on our samples before aging. The C 1 s spectrum of pristine carbon-free $LiFePO_4$ is dominated by contamination carbon (284.6 eV) with a minority contribution from oxygenated carbon at the extreme surface of the active material (286 and 289.4 eV). The absence of the characteristic peak at 290 eV confirms the absence of surface Li_2CO_3 on our samples [13,20]. The only noticeable difference in XPS results between both samples was the extremely important atomic percentage of carbon (83%) due to the carbon coating, compared to the 9% obtained for the carbon-free material.

For $LiFePO_4$–C, after 1 month of contact with $LiPF_6$ EC/DMC electrolyte at 25 °C, only very low amount of products coming from the decomposition of organic solvent such as alkyl carbonates $ROCO_2Li$ (286–288 eV and 288–291 eV [20,33,34]) and/or compounds with ether function (286–288 eV [35]) were evidenced from the analysis of the C 1s spectrum (Fig. 8a and Table 1).

The two F 1s main peaks indicate the presence of fluorine under at least two forms assigned to LiF (685–686.2 eV [34,36–39]) and $Li_xPF_y/Li_xPO_yF_z$ (687–688 eV [20,36,37]) (Fig. 8b), compounds already observed in previous studies [20]. However, based only on F 1s spectrum, it is not possible to completely rule out the presence of some $LiPF_6$ traces (686–687.9 eV [37,39]. P2p spectra (not shown) did not bring further information as the binding energies of P–F bonds in $LiPF_6$ (136.5–138.2 eV [39]) and Li_xPF_y (137 eV [20]) are overlapping. Consequently such data are not reported in Table 1.

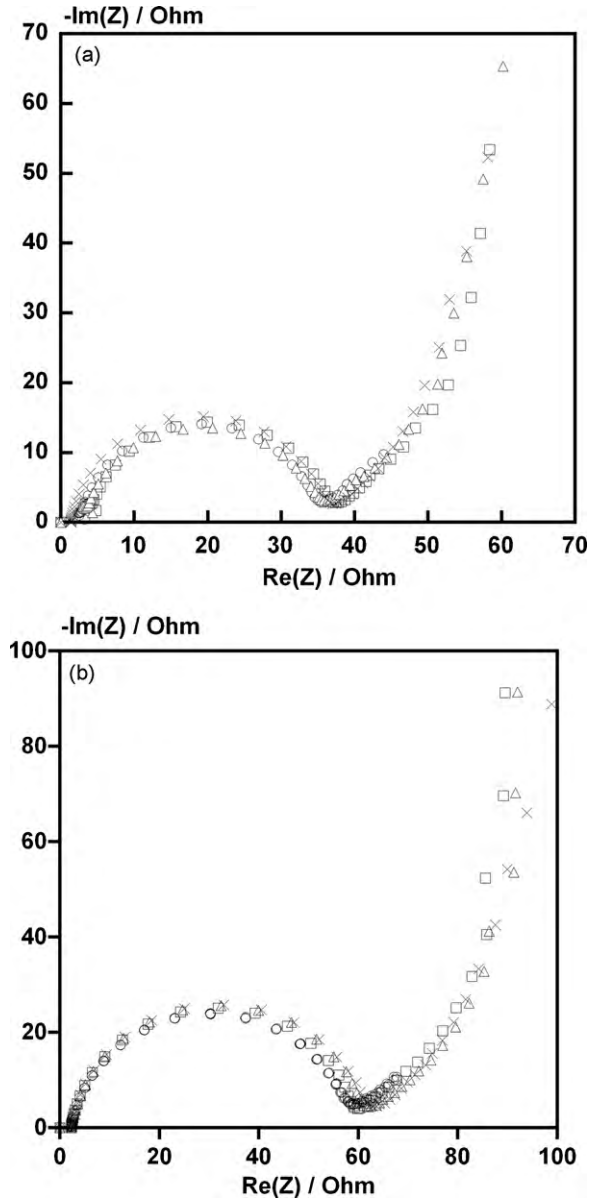

Fig. 7. Nyquist diagrams at 25 °C for $LiFePO_4$–C (a) and $LiFePO_4$ (b) electrodes immediately after assembling the cell (circles), and after 1 h (squares), 3 days (triangles) and 2 weeks (crosses) in $LiPF_6$ 1 M in EC/DMC.

The apparition of fluorine and of new organic carbon species confirms the covering of the material surface by an interphase layer in agreement with NMR data. The amount of carbon assigned to the coating (284.6 eV) decreases from 83% to 45% (Table 1), while the amount of PO_4 and Fe assigned to the underlying $LiFePO_4$ material is low and cannot be determined precisely. It shows that the growing surface layer appears mainly onto the carbon surface coating.

Concerning $LiFePO_4$ samples without carbon coating, an overall similar behavior can be observed. The atomic percentage of the carbon at 285 eV, detected on the pristine material decreases from 18% to 9% (Table 1). In the same time, a slight increase of new carbon peaks ($ROCO_2Li$ 286–288 eV and 288–291 eV) already observed for $LiFePO_4$–C and the apparition of fluorine (LiF and $Li_xPF_y/Li_xPO_yF_z$) confirm the covering of the material by an interphase layer. The amount of PO_4 and Fe assigned to the underlying $LiFePO_4$ material decreases after electrolyte immersion. It indicates that the surface layer appears onto the $LiFePO_4$ surface as well.

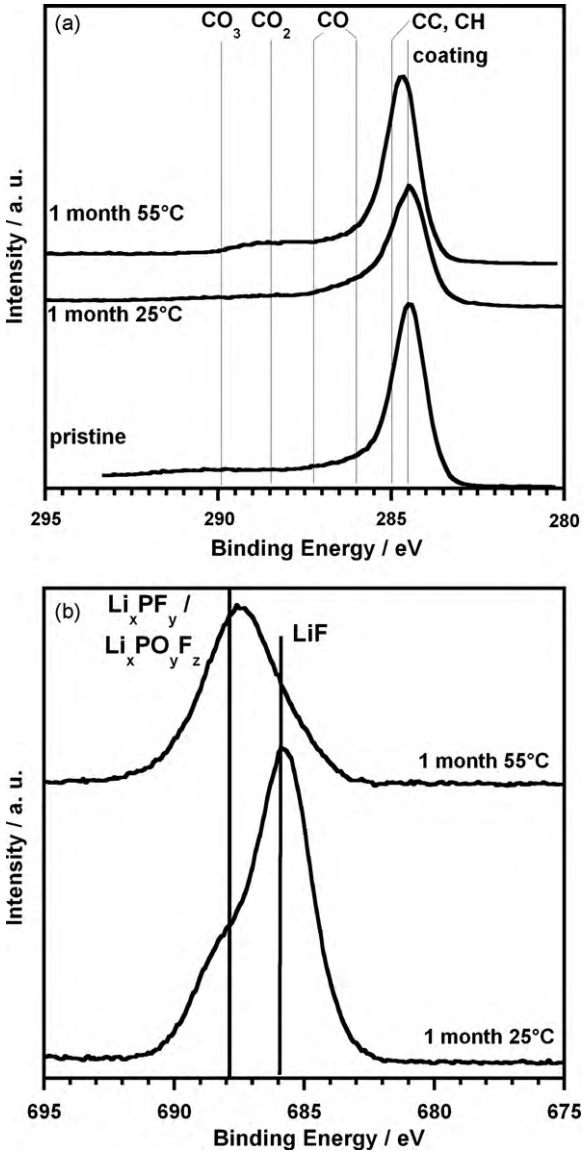

Fig. 8. XPS C 1s (a) and F 1s (b) spectra for pristine $LiFePO_4$–C (only shown in a), and after 1 month of contact at 25 °C and 55 °C in $LiPF_6$ 1 M in EC/DMC electrolyte.

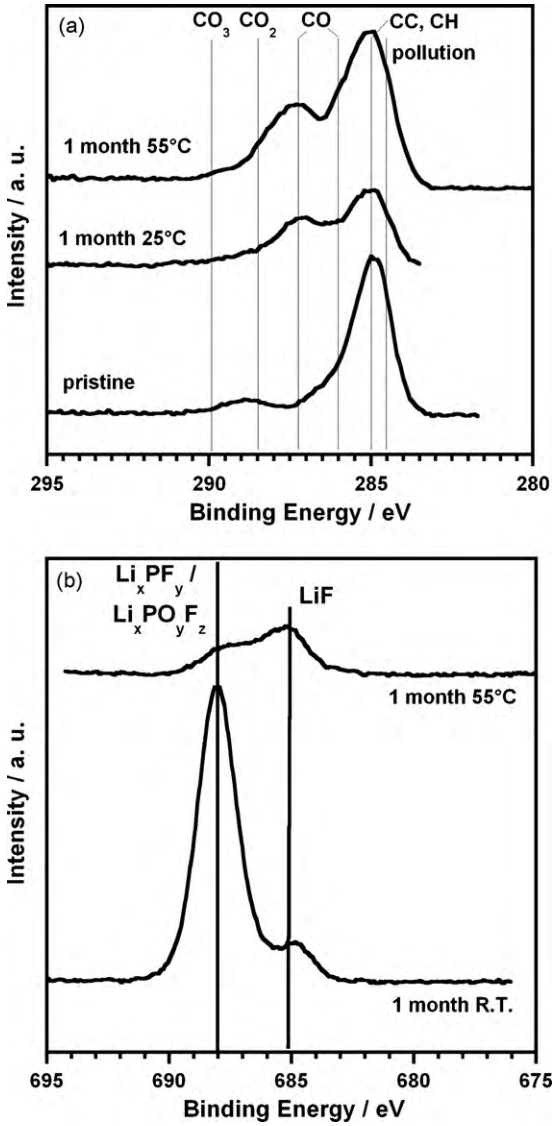

Fig. 9. XPS C 1s (a) and F 1s (b) spectra for pristine $LiFePO_4$ (only shown in a), and after 1 month of contact at 25 °C and 55 °C in $LiPF_6$ 1 M in EC/DMC electrolyte.

Table 1
Binding energies and atomic percentages deduced from the fit of XPS spectra of $LiFePO_4$ and $LiFePO_4$–C, pristine, after 1 month of contact with $LiPF_6$ 1 M in EC/DMC at 25 °C and 55 °C.

Element	BE (eV)	Attributed species	$LiFePO_4$–C			$LiFePO_4$		
			Pristine	25 °C	55 °C	Pristine	25 °C	55 °C
C	284.6	Pollution/coating	83%	45%	46%	9%	n/a	n/a
	285	CC–CH		8.5%	19.5%	18%	9%	21%
	286	CO	6.5%	6.5%	6%	3%	2%	6%
	287.2	CO		3.5%	3.5%		4.5%	<1%
	288.5	CO_2		1.5%	4.5%	1%	1%	10.5%
	289.4	CO_3	<1%	1%	1%		0.5%	1%
O	531.5	PO_4	7%	9%	7%	52.5%	36%	23.5%
	533	CO–OH	1.5%	4.5%	3.5%	7%	13.5%	23%
P	133.5	PO_4	1%	1%	1.5%	9.5%	5%	4%
	135.5	PO–PF		1.5%	0.5%		4.5%	3%
F	685	LiF		11%	2%		3%	3%
	688	$Li_xPO_yF_z/Li_xPF_y$		6%	4%		18%	1%
Fe	709–712	Fe^{II}/Fe^{III}	1%	1%	1%	9%	3%	4%

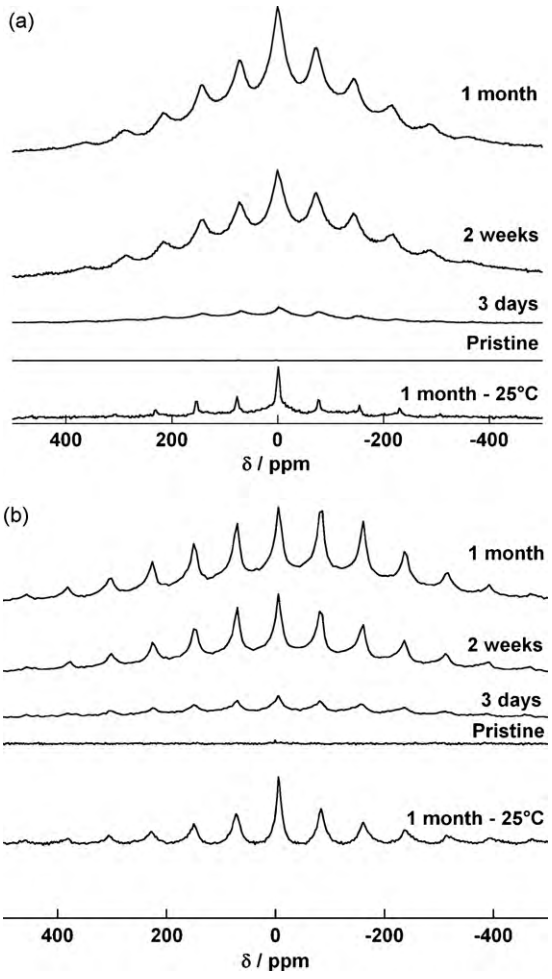

Fig. 10. Normalized ^{7}Li MAS NMR spectra of $LiFePO_4$–C (a) and $LiFePO_4$ (b) soaked in $LiPF_6$ 1 M in EC/DMC for 1 month at 25 °C and for various durations at 55 °C.

3.3. Aging at 55 °C

The ^{7}Li MAS NMR spectra acquired for $LiFePO_4$–C samples soaked in electrolyte for various durations are compared to those obtained at ambient temperature for 1 month in Fig. 10. The storage at higher temperature clearly aggravates the reaction of formation of the interphase as it can be seen from the dramatic increase of intensity on the corresponding NMR spectra. Indeed, the signal strongly and continuously grows from 3 days contact to 1 month contact. The corresponding integrated intensity is multiplied by a factor of 3.2 from 3 days to 2 weeks and by a factor of 1.4 from 2 weeks to 1 month (Fig. 5). This indicates that even after 1 month at 55 °C, the formation of interphase still goes on, although it seems to slow down. It confirms the extremely slow kinetics for the passivation reaction of the surface of the electrode.

In addition, concerning the spectra at 55 °C, an important change in the overall lineshape is observed. This modification comes mostly from an increase in the line width of the resonance resulting in a much broader line shape. In addition, it not possible to rule out the contribution of an additional and most probably unresolved signal, centred at approximately 0 ppm and adding intensity to the observed spectra. These two phenomena may be the results of an increased interaction between some of the detected nuclear spins of Li nuclei and electronic spins of paramagnetic centres at the surface of the electrode material or even trapped in the interphase.

A similar phenomenon of aggravation of surface species formation is observed, as expected, for the non-carbon-coated material. The spectra shown in Fig. 10 indicate an important increase in NMR signal intensity after 3 days of contact. For instance, the integration of the intensity of the signal gives a ratio of 4.2 between the $LiFePO_4$ samples soaked in electrolyte for 3 days at 25 and 55 °C, showing an even stronger effect of the temperature for a material not protected by a carbon coating. Moreover, the important difference of intensity between the carbon-coated and the carbon-free material even at 55 °C (Fig. 5), supports the protective role of the carbon-coated on the surface of the electrode material towards reactions with the electrolyte. In particular, the protective effect of the carbon coating, again, counteracts an expected higher surface reactivity due to a smaller grain size. A ratio of 1.2 between $LiFePO_4$ samples soaked in electrolyte for three days at 55 °C and 1 month at 25 °C (Figs. 5 and 10), confirms that complete passivation was not reached after one month at 25 °C.

In addition, the increase of the width of the line shape is even more visible for the carbon-free sample and in particular for the sample soaked for 1 month. According to previously published data for $LiNi_{1/2}Mn_{1/2}O_2$ material [23], it shows that an increase in temperature leads not only to an increase of the amount of lithium-containing species on the surface of the grains but also to a different interaction between lithium nuclei in the interphase and the underlying paramagnetic material. In the present case, the stronger interaction between lithium nuclei in the interphase and iron paramagnetic centres could be caused by the presence of iron coming from a partial dissolution of the $LiFePO_4$ [13,40,41] and trapped in the interphase or a more intimate contact between the interphase and the surface of $LiFePO_4$. ICP performed on $LiFePO_4$–C and $LiFePO_4$ samples after aging at 55 °C for 1 month showed that iron dissolution is occurring. The amount of dissolved iron was found to be respectively 6–7 and 14–15 at.%, which correlate well with results obtained by Koltypin et al. [42]. Mössbauer spectroscopy performed on samples aged at 55 °C indicates a significant increase in Fe^{3+} content (Fig. 11 and Table 2) although trivalent iron was already detected at 25 °C in much smaller amounts. The larger amount of Fe^{3+} in the case of $LiFePO_4$ (40% of total iron) compared to $LiFePO_4$–C (18% of total iron) follows the same trend as that of ICP analysis and suggests again a dominating effect of the protective role of the carbon coating versus an enhanced surface reactivity due to a smaller grain size and higher specific surface for the carbon-coated material. The broad peaks, deviating from Lorentzian profile, observed for the Fe^{3+} contribution ($\delta \approx 0.43$ mm s^{-1}, $\Delta \approx 0.52$ mm s^{-1}, $\Gamma \approx 0.5$ mm s^{-1}) are characteristic of heterogeneous environment around the Fe^{3+} ions at the local scale, and can be a sign of a highly disordered or amorphous phase. The Fe^{2+} component of the Mössbauer spectrum corresponds to an oxygen octahedral environment, which associated parameters are well defined and correspond to the $LiFePO_4$ olivine environment ($\delta \approx 1.22$ mm s^{-1}, $\Delta \approx 2.97$ mm s^{-1}, $\Gamma \approx 0.31$ mm s^{-1}) [7]. Although it is not possible to determine from Mössbauer whether the formed Fe^{3+} is trapped in the interphase or present within the active material, it is reasonable to correlate the increase in paramagnetic Fe^{3+} with the increase of the width of the NMR line shape.

Table 2
Fe^{2+} and Fe^{3+} content obtained from Mössbauer experiments for $LiFePO_4$–C and $LiFePO_4$ pristine, soaked in $LiPF_6$ 1 M in EC/DMC for 1 month at 25 °C and 55 °C.

	Fe^{2+} content	Fe^{3+} content
$LiFePO_4$–C		
Pristine	94%	6%
25 °C	90%	10%
55 °C	82%	18%
$LiFePO_4$		
Pristine	97%	3%
25 °C	92%	8%
55 °C	60%	40%

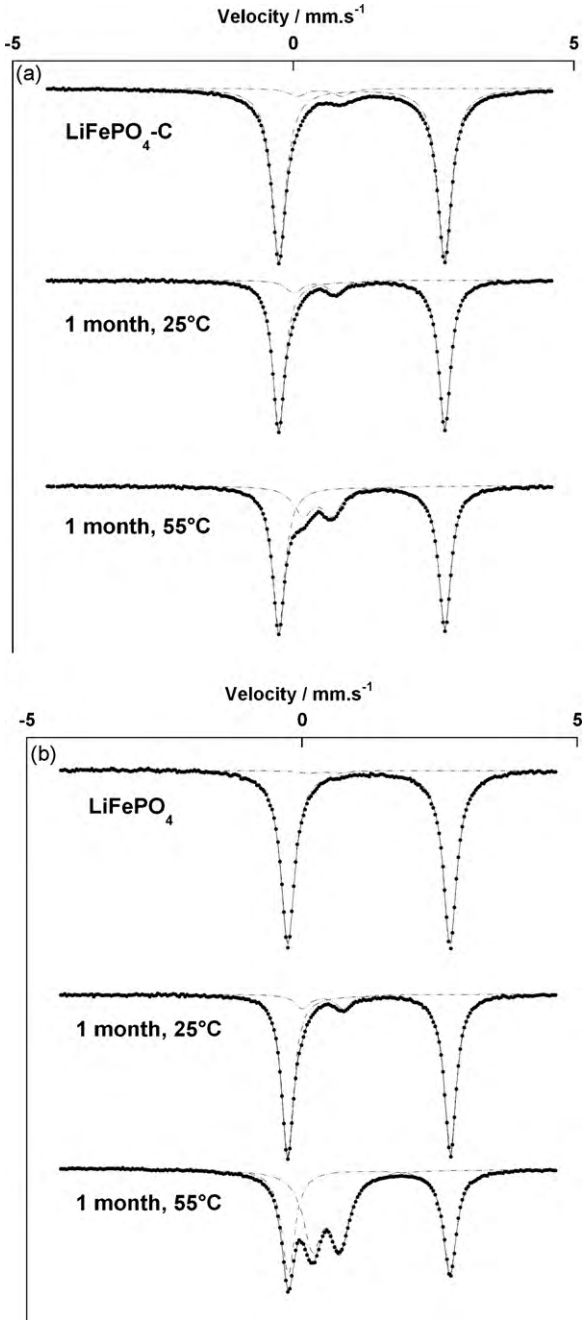

Fig. 11. Mössbauer spectra of $LiFePO_4$–C (a) and $LiFePO_4$ (b) pristine, soaked in $LiPF_6$ 1 M in EC/DMC for 1 month at 25 °C and 55 °C.

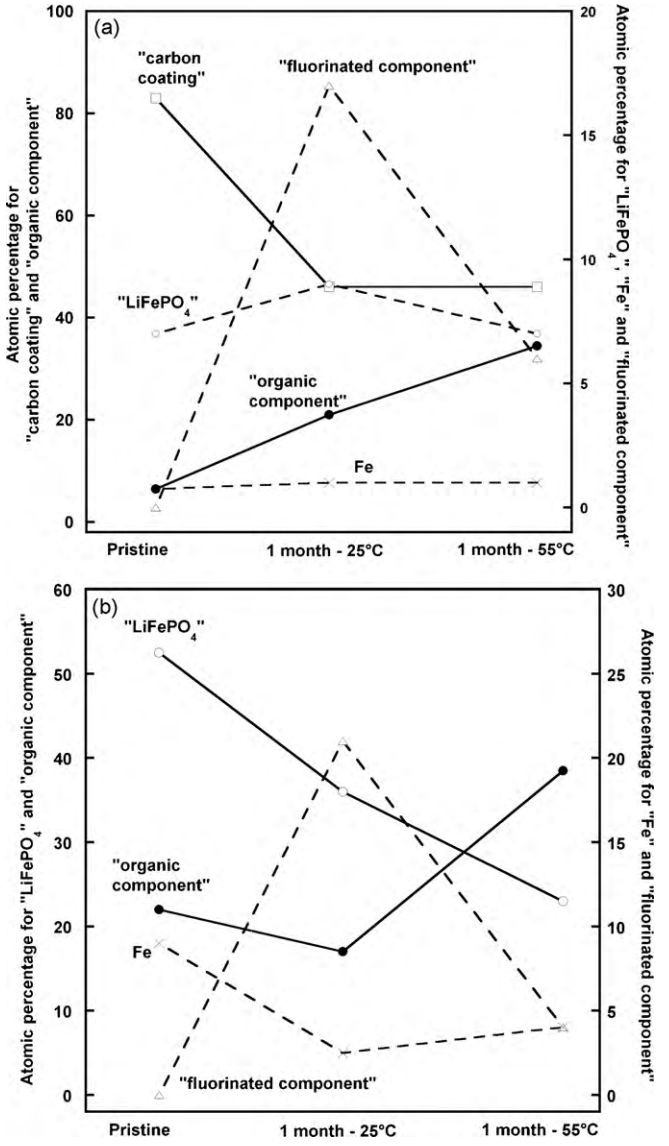

Fig. 12. Atomic percentages deduced from XPS analysis for $LiFePO_4$–C (a) and carbon-free $LiFePO_4$ (b) for pristine samples, and samples soaked in $LiPF_6$ 1 M in EC/DMC electrolyte for 1 month at 25 °C and 55 °C. For clarity, O 1s at 531.5 eV (open circles) is labelled "LiFePO4", C 1s at 284.6 eV (open squares) is labelled "carbon coating", C 1s at 285–287.2 eV (black dots) is labelled "organic component", F 1s at 685–688 eV (open triangles) is labelled "fluorinated component", and Fe 2p3/2 at 709–712 eV (crosses) is labelled "Fe". Lines corresponds to the left-hand scale and dashes correspond to the right-hand scale.

In the case of a simple growth of the interphase on the surface of the electrode material without the inclusion of paramagnetic centres within, a sharpening of the line shape of NMR spectra would be expected along the increase in intensity, due to the stacking of additional diamagnetic lithium species [22] further from the paramagnetic $LiFePO_4$. This is not the case here and these results show that the architecture of the interphase drastically changes when the temperature is raised to 55 °C. Most probably, both phenomena, iron trapping and modification of the interphase are occurring.

In order to detect such modifications, XPS experiments have been performed on the $LiFePO_4$ samples soaked in electrolyte at 55 °C. Concerning the carbon-free $LiFePO_4$, XPS measurements allow observing the same lithiated species as those found at 25 °C (Fig. 9). The evolution of the atomic percentage of carbon, F (685 and 688 eV), Fe (709–712 eV) and O (531.5 eV) are displayed in Fig. 12a. For clarity purpose, the percentages of other species are not displayed in Fig. 12 but can be found in Table 1. The continuous decrease observed for PO_4 phosphorus (not shown in figure) and oxygen from pristine to 1 month contact at 25 °C and 55 °C indicates unambiguously the more important covering of the material surface when the temperature is raised, consistent with NMR results. This evolution is explained by the increase of the atomic percentage of fluorine attributed to the covering of the carbon-free $LiFePO_4$ by inorganic lithiated species (LiF, Li_xPF_y and $LiPO_yF_z$) in the case of the sample soaked at 25 °C. Comparing now carbon-free $LiFePO_4$ samples soaked at 25 °C and 55 °C, the apparent decrease of the atomic percentage of fluorine concomitant with the increase of the amount of carbon-based species suggests further covering of the surface of the electrode involving organic species stacked on the top of LiF and $LiPO_yF_z$ type products.

In addition, concerning the evolution of the atomic percentage of iron, the concomitant decrease of iron, oxygen when $LiFePO_4$ is stored in electrolyte at 25 °C is consistent with a simple covering of the surface of the electrode material by decomposition products from the electrolyte. In the case of a storage at 55 °C, although the atomic percentage of O further decreases, in agreement with the more important covering deduced from NMR data, an opposite evolution is observed for iron as the atomic percentage doubles.

Comparing with the evolution of the $LiFePO_4$–C sample soaked for 1 month at 55 °C, an overall similar evolution is observed. When the temperature is increased from 25 °C to 55 °C, atomic percentage of fluorine assigned to LiF, Li_xPF_y and $LiPO_yF_z$ are lower and the carbon contributions higher suggesting a covering of inorganic surface species by organic products coming from the decomposition of the electrolyte solvents. For C-coated soaked at 55 °C, analysis of surface Fe is not precise enough and does not allow concluding on trapped Fe in the interphase layer, as the spectrum is dominated by carbon of carbon coating.

Concerning $LiFePO_4$–C, the amount of C assigned to the carbon coating (284.6 eV) does not increase with the temperature. Nevertheless, this contribution can overlap with contributions of other types of carbon with close binding energies. Then, it seems difficult to rely only on the evolution of the signal at 284.6 eV to reflect the real evolution of the surface of the electrode material. The concomitant strong increase of the amount of lithiated surface species observed by ^{7}Li NMR, when the temperature is increased from 25 °C to 55 °C suggests a stacking of interphase species on top of each other instead of a covering of the whole surface. In parallel, O and Fe contributions attributed to the $LiFePO_4$ do not change significantly and although quite low, they are still detectable after a long contact time with the electrolyte at 55 °C. It supports also the fact that surface species are present mostly on the carbon coating.

Fig. 13a and b shows the evolution of in situ electrochemical impedance of the $LiFePO_4$–C and $LiFePO_4$ electrodes respectively, in open circuit at 55 °C. For both samples, a decrease in the interfacial resistance is first noticed when the temperature has risen to 55 °C. This behaviour is attributed to the temperature dependence of the electric conductivity of the electrode. For $LiFePO_4$–C, from 3 days on, the resistance increases but no new semi-circle is detected. The evolution in the interfacial resistance values indicates clearly the deterioration of the electrode performance in the electrolyte at high temperature. This increase of the overall resistance and the lower specific capacity could correspond to phenomena such as loss of electrical contact between grains of active material, iron dissolution in the electrolyte [13,41,42] or the presence of a resistive interphase with a time constant close to that of the charge transfer phenomenon. Although iron dissolution is observed by ICP, the 7 and 15% of atomic Fe dissolution cannot account for the respective 25 and 21% initial capacity loss observed for the cycling experiments of electrodes that have been exposed to electrolyte at 55 °C. Electrodes used for impedance measurement have been recovered and pressed at 3 tons before a last measurement (Fig. 13). A clear change is noticed with a smaller overall resistance, showing that the contribution of intergrain contact is not negligible anymore. This result shows that in addition to iron dissolution, long contact at high temperature leads to degradation of electrical contact in the electrodes. If the presence of a resistive film on the surface of $LiFePO_4$ grains were the dominating process, no change would be observed after pressing the electrode. Moreover, the amount of interphase (Fig. 5) of $LiFePO_4$ after 1 month at ambient temperature and $LiFePO_4$–C after 1 month at 55 °C, are of the same order of magnitude and the detected species are the same, as deduced from XPS analysis. This suggests that the presence of the detected species on the surface of the electrode materials does not lead to the observed increase of the resistance on EIS spectra and the lower specific capacity. Again, it is not possible to completely rule out a minor contribution of a resistive film with a time constant close to that of the charge transfer phenomenon but the degradation of the electrochemical performance does not seem to be related to a resistive contribution of the interphase.

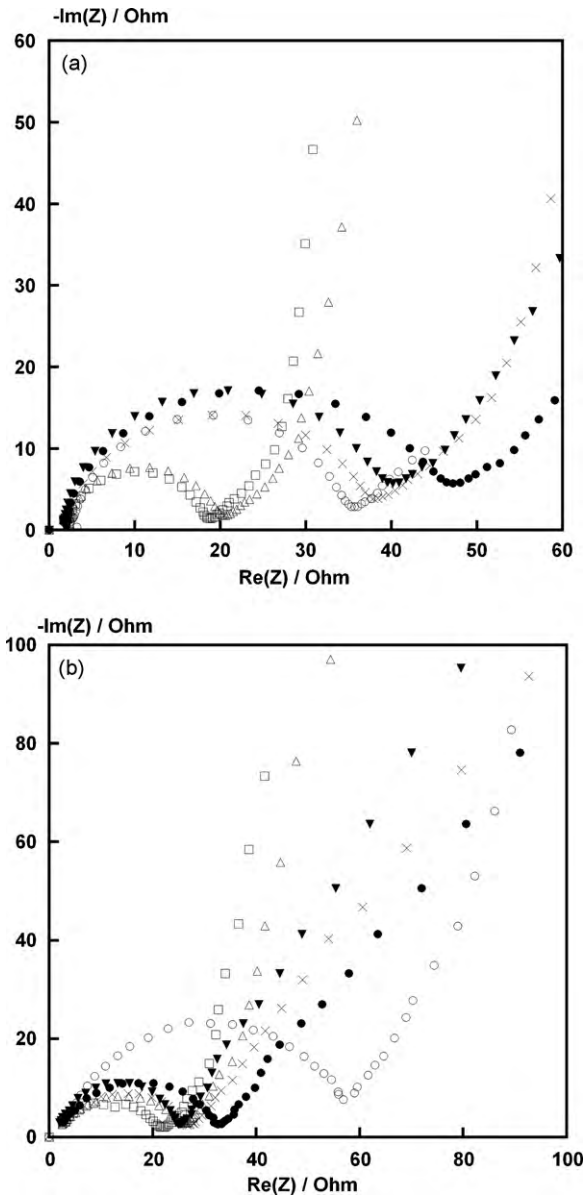

Fig. 13. Nyquist diagrams immediately after assembling the cell at 25 °C (circles), and at 55 °C after 1 h (squares), 3 days (triangles), 2 weeks (crosses), 1 month (dots) and 1 month followed by pressing under 3 tons (black triangles) for a $LiFePO_4$–C electrode (a) and for a $LiFePO_4$ electrode (b) in $LiPF_6$ 1 M in EC/DMC.

Electrodes stored for one month in the electrolyte at 55 °C have been recovered, rinsed in order to remove the surface species and cycled at ambient temperature with fresh electrolyte (Fig. 3). The mass of active material was measured before the storage step in order to compare the specific capacities with those of cycled pristine electrodes. The lower specific capacity observed for the soaked sample is also in agreement with the degradation of the electrode along the storage but no further alteration of the performance is noticed along the cycling at ambient temperature. These results are also consistent with both a loss of some of the electrical contacts as well as the dissolution of iron during the storage. In the case of a dominating influence of a resistive film on the surface on the electrochemical performance, removed by rinsing, a specific capacity close to that of the pristine material would be recovered. It is

therefore reasonable to assume that the degradation of the electrochemical performance is not caused by a resistive contribution of surface species.

Similar results are observed for carbon-free $LiFePO_4$ although the increase in the interfacial resistance is less pronounced (Fig. 13b). The accelerated aging observed for the carbon-coated material might be related to the combination of its higher specific surface and the increased temperature. The interphase deposits on the carbon coating in the case of $LiFePO_4$–C could make this material more sensitive to the formation of interphase due to a more sensible loss of electrical contact between the particles within the composite electrode. This phenomenon would explain the more important degradation of the electrode made with the carbon-coated $LiFePO_4$ observed via electrochemical measurements.

These results suggest that the species detected on the surface of the grains of active material using ^{7}Li MAS NMR have a very limited effect on the electrochemical properties of the electrode material. Very little effect has been observed on the respective specific capacities of $LiFePO_4$ and $LiFePO_4$–C after a 1 month storage at ambient temperature even though the amount of detected surface species is 8 times higher in the case of the non-carbon-coated material. These results indicate that the amount of interphase is not a parameter limiting the performance of the material or that surface species are not in amount large enough to form a resistive barrier to lithium transfer from the electrolyte to $LiFePO_4$.

4. Conclusions

The formation and the growth of surface species coming from reaction with $LiPF_6$ electrolyte have been followed successfully using ^{7}Li MAS NMR in the case of $LiFePO_4$ obtained by two different synthesis routes leading to a carbon-coated material and a non-coated material displaying a larger grain size.

^{7}Li MAS NMR experiments on samples soaked in electrolyte at 25 °C permit to observe the growth of an interphase with a clear increase in lithiated species as a function of contact duration. The reaction is significantly aggravated in the case of the non-carbon-coated material despite the smaller grain size, the higher specific surface area and the rougher surface of the carbon-coated $LiFePO_4$. These results demonstrate the clear influence of the carbon coating as a protection against parasitic reaction with the electrolyte.

For both types of $LiFePO_4$, the interphase grows continuously as no passivation state is reached after one month of contact with the electrolyte contrasting with the behavior of oxides such as $LiNi_{0.5}Mn_{0.5}O_2$ which reaction with the electrolyte is extremely fast and occurs during the first moments of exposure [24]. XPS experiments allowed analyzing the chemical composition of the interphase and indicated the presence of mainly inorganic products coming from the decomposition of the $LiPF_6$ salt. The interphase formed does not lead to a resistive film that would hinder the electrochemical performance of the electrode. This result indicates that the interphase seems to have a very limited influence of the electrode behavior at 25 °C. When the temperature is increased to 55 °C, the amount of lithiated species detected on the surface of the electrode material increases dramatically but yet, no passivation state is reached within 1 month although the reaction seems to slow down. These results show that the reaction of interphase formation in the electrolyte must have a very slow kinetics. In addition, XPS shows that the higher temperature promotes the formation of organic species on the surface, although LiF, Li_xPF_y and $LiPO_yF_z$ are still detected. Nevertheless, no evidence of the formation of a resistive film is found and the evolution deduced from EIS measurements suggests only a deterioration of the electrode, assigned to iron dissolution and loss of electrical contact within the electrode. This result confirms the very limited role of the interphase on the electrochemical performance of $LiFePO_4$ electrodes as opposed to the behavior of most oxides used as electrode materials in Li-ion batteries. Nevertheless, the interphase deposits on the carbon coating in the case of $LiFePO_4$-C seems to make this material more sensitive to the formation of interphase to be linked to the more important degradation of the electrode observed via electrochemical measurements. Then, the interphase growth can accelerate the degradation of the electrochemical performance by achieving an accelerated loss of electrical contact within the electrode.

Acknowledgements

The authors wish to thank Dr. Danielle Gonbeau and Dr. Remi Dedryvère for helpful discussion on XPS analysis and Dr. Michel Suchaud for Mössbauer experiments. Financial support of the Ph.D. of Jean-Frédéric Martin from the Region Pays de la Loire is gratefully acknowledged.

References

[1] H. Huang, S.C. Yin, L.F. Nazar, Electrochem. Solid-State Lett. 4 (10) (2001) A170.
[2] C.H. Mi, G.S. Cao, X.B. Zhao, Mater. Lett. 59 (1) (2005) 127.
[3] N.J. Yun, H.W. Ha, K.H. Jeong, H.Y. Park, K. Kim, J. Power Sources 160 (2) (2006) 1361.
[4] R. Dominko, M. Bele, M. Gaberscek, M. Remskar, D. Hanzel, S. Pejovnik, J. Jamnik, J. Electrochem. Soc. 152 (3) (2005) A607.
[5] S.Y. Chung, J.T. Bloking, Y.M. Chiang, Nat. Mater. 1 (2) (2002) 123.
[6] C. Delacourt, L. Laffont, R. Bouchet, C. Wurm, J.B. Leriche, M. Morcrette, J.M. Tarascon, C. Masquelier, J. Electrochem. Soc. 152 (5) (2005) A913.
[7] A. Yamada, S.C. Chung, K. Hinokuma, J. Electrochem. Soc. 148 (3) (2001) A224.
[8] Y. Sundarayya, S.K.C. Kumara, C.S. Sunandana, Mater. Res. Bull. 42 (11) (2007) 1942.
[9] D. Aurbach, M.D. Levi, E. Levi, H. Teller, B. Markovsky, G. Salitra, U. Heider, L. Heider, J. Electrochem. Soc. 145 (9) (1998) 3024.
[10] E. Ericksson, Ph.D. Thesis, Uppsala University, 2001.
[11] T. Eriksson, Comprehensive Summaries 651, Faculty of Science and Technology of Uppsala, 2001.
[12] Y. Matsuo, R. Kostecki, F. McLarnon, J. Electrochem. Soc. 148 (7) (2001) A687.
[13] D. Aurbach, B. Markovsky, G. Salitra, E. Markevich, Y. Talyossef, M. Koltypin, L. Nazar, B. Ellis, D. Kovacheva, J. Power Sources 165 (2) (2007) 491.
[14] M. Koltypin, D. Aurbach, L. Nazar, B. Ellis, J. Power Sources 174 (2) (2007) 1241.
[15] M. Kerlau, R. Kostecki, J. Electrochem. Soc. 153 (9) (2006) A1644.
[16] T. Matsushita, K. Dokko, K. Kanamura, J. Electrochem. Soc. 152 (11) (2005) A2229.
[17] H. Ota, T. Akai, H. Namita, S. Yamaguchi, M. Nomura, J. Power Sources 119–121 (2003) 567.
[18] B.J. Neudecker, R.A. Zuhr, B.S. Kwak, J.B. Bates, J.D. Robertson, J. Electrochem. Soc. 145 (12) (1998) 4148.
[19] J.C. Dupin, D. Gonbeau, H. Benqlilou-Moudden, Ph. Vinatier, A. Levasseur, Thin Solid Films 384 (2001) 23.
[20] K. Edström, T. Gustafsson, J.O. Thomas, Electrochim. Acta 50 (2–3) (2004) 397.
[21] M. Herstedt, M. Stjerndahl, A. Nyten, T. Gustafsson, H. Rensmo, H. Siegbahn, N. Ravet, M. Armand, J.O. Thomas, K. Edström, Electrochem. Solid-State Lett. 6 (9) (2003) A202.
[22] N. Dupré, J.F. Martin, D. Guyomard, A. Yamada, R. Kanno, J. Mater. Chem. 18 (2008) 4266.
[23] N. Dupré, J. Oliveri, J.-F. Martin, P. Soudan, A. Yamada, R. Kanno, D. Guyomard, Electrochem. Commun. 10 (12) (2008) 1897.
[24] N. Dupré, J. Oliveri, J.-F. Martin, P. Soudan, A. Yamada, R. Kanno, D. Guyomard, J. Electrochem. Soc. 156 (5) (2009) C180.
[25] N. Dupré, J.F. Martin, D. Guyomard, A. Yamada, R. Kanno, J. Power Sources 189 (2009) 557.
[26] R. Dominko, J.M. Goupil, M. Bele, M. Gaberscek, M. Remskar, D. Hanzel, J. Jamnik, J. Electrochem. Soc. 152 (5) (2005) A858.
[27] M. Ménétrier, C. Vaysse, L. Croguennec, C. Delmas, C. Jordy, F. Bonhomme, P. Biensan, Electrochem. Solid-State Lett. 7 (6) (2004) A140.
[28] A.K. Padhi, J.B. Goodenough, J. Electrochem. Soc. 144 (4) (1997) 1188.
[29] A. Yamada, S.C. Chung, J. Electrochem. Soc. 148 (2001) A960.
[30] N. Dupré, J. Oliveri, J. Degryse, J.F. Martin, D. Guyomard, Ionics 14 (3) (2008) 203.
[31] M.C. Tucker, M.M. Doeff, T.J. Richardson, R. Finones, J.A. Reimer, E.J. Cairns, Electrochem. Solid-State Lett. 5 (5) (2002) A95.
[32] N. Dupré, C.P. Grey, Chem. Rev. 104 (10) (2004) 4493.
[33] V. Eshkenazi, E. Peled, L. Burstein, D. Golodnitsky, Solid State Ionics 170 (2004) 83.
[34] R. Dedryvère, S. Laruelle, S. Grugeon, L. Gireaud, J.M. Tarascon, D. Gonbeau, J. Phys. Chem. B 109 (2005) 15868.
[35] S.H. Kang, D.P. Abraham, A. Xiao, B.L. Lucht, J. Power Sources 175 (2008) 526.
[36] D. Aurbach, Nonaqueous Electrochemistry, Marcel Dekker Inc., New York, 1999.

[37] D. Aurbach, A. Zaban, Y. Gofer, Y. Ein Ely, I. Weissman, O. Chusid, O. Abramson, J. Power Sources 54 (1995) 76.
[38] K. Kanamura, H. Tamura, Z.I. Takehara, J. Electroanal. Chem. 33 (1992) 127.
[39] A. Nyten, M. Stjerndahl, H. Rensmo, H. Siegbahn, M. Armand, T. Gustafsson, K. Edström, J.O. Thomas, J. Mater. Chem. 16 (2006) 3483.
[40] S. Leroy, H. Martinez, R. Dedryvère, D. Lemordant, D. Gonbeau, Appl. Surf. Sci. 253 (2007) 4895.
[41] N. Tchev, Y. Chen, S. Okada, J. Power Sources (2003) 749.
[42] M. Koltypin, D. Aurbach, L. Nazar, B. Ellis, Electrochem. Solid-State Lett. 10 (2) (2007) A40.